J Mater Sci (2009) 44:849–854
DOI 10.1007/s10853-008-3137-5

Preparation and electrical conductivity of SiO_2/polypyrrole nanocomposite

Qunwei Tang · Xiaoming Sun · Qinghua Li · Jianming Lin · Jihuai Wu

Received: 23 September 2008 / Accepted: 25 November 2008 / Published online: 11 December 2008

Abstract In the present study we have chemically polymerized silica/polypyrrole (SiO_2/PPy) nanocomposite in the presence of sodium dodecyl benzene sulfate (SDBS) as dopant and iron chloride ($FeCl_3$) as oxidant. The SiO_2/PPy nanocomposite presents an electrical conductivity of 32.41 S cm^{-1} and percolation threshold of 20 wt%. The resulting SiO_2/PPy nanocomposites have been extensively characterized in terms of their molecular structure, particle size, morphology, stability, and electroactivity. These SiO_2/PPy particles have a rather polydisperse morphology. The effects of synthesis parameters such as oxidant, PPy, SDBS, reaction temperature and time, on the electrical conductivity of the nanocomposite have been detailedly optimized. And the conducting nanocomposite presented a good environmental stability.

Introduction

One of the current interests in research on nanostructured materials is the preparation of nanocomposite conducting colloidal particles consisting of inorganic component and conducting polymers. The optical and electrical properties of these materials differ from their individual nanoparticles or macroscopic equivalents. Therefore they can be effectively applied in the fields of sensors, optics, and electronics. Techniques for the preparation of nanocomposites containing conducting polymers have been reviewed [1].

Conducting polymers such as polypyrrole (PPy) have attracted considerable attention in the past two decades for their potential applications in electromagnetic radiation shielding, microwave absorbent and battery, et al. [2–5]. Of all known conducting polymers, PPy has been an object of intense investigation because of its good conductivity, stability in air, interesting electrochemical behavior, corrosion protection, and ease of preparation [6]. It can be prepared by two main routes, the chemical [7, 8] and the electrochemical [9] oxidation of pyrrole in organic solvents and in aqueous media. As known, the conductivity of PPy can be attributed to the hop electrons along and across the polymer chains with the conjugating bonds [10]. Owing to the preparation method and doping, the conductivity of PPy can be improved heavily to an attractive level [11–13].

Conducting polymer-based nanocomposites decorated with oxides or metallic nanoparticles provide exciting systems to investigate with the possibility of designing device functionality. There have been numerous publications describing the preparation of inorganic–organic hybrid materials which contain PPy as the organic component. For example, Partch et al. have described the preparation of several PPy-coated inorganic oxide composites by utilizing the inorganic oxide as a colloidal oxidant [14]. Mehrotra et al. have synthesized PPy-silica "hybrid glasses" by the in situ chemical polymerization of pyrrole in a host glass matrix containing copper ions [15]. Yoneyama and co-workers have incorporated a wide range of particulate inorganic oxides such as titanium oxide, tungsten oxide, and manganese oxide into electrochemically synthesized thin films of PPy [16]. In addition, Yamamoto's group have synthesized organic–organic hybrid particles which are apparently colloidally stable by polymerizing pyrrole onto the surface of poly(styrene-co-butadiene) latexes [17]. There are other studies on synthesis, characterization and application of

---

Q. Tang · X. Sun · Q. Li · J. Lin · J. Wu (✉)
The Key Laboratory for Functional Materials of Fujian Higher Education Institute of Material Physical Chemistry, Huaqiao University, Quanzhou 362021, China
e-mail: jhwu@hqu.edu.cn

nanocomposites with diverse combinations of PPy and inorganic nanoparticles, such as PPy/carbon nanotubes [18, 19], PPy/clay [20, 21], PPy/metal [22], PPy/oxide [23], PPy/zeolite [24, 25].

In the article, we reported a SiO_2/polypyrrole (SiO_2/PPy) nanocomposite with a conductivity of 32.41 S cm^{-1} prepared by aqueous solution polymerization in the presence of sodium dodecyl benzene sulfate (SDBS) and iron chloride ($FeCl_3$). Effects of preparation conditions such as $FeCl_3$, PPy, SDBS, reaction time and temperature on conductivity of the nanocomposites were investigated. The morphology, molecular structure and electrochemical property of the nanocomposites were characterized using scanning electron microscopy (SEM), infrared spectrum (FTIR), and cyclic voltammetry (CV), respectively.

Experimental

Materials

Pyrrole (Py) monomer was distilled under reduced pressure prior to use. $FeCl_3$ was used as a radical oxidant for the synthetic reaction of PPy. SiO_2 ultrafine powder (8–10 nm, 0.75–1.0 mL/g, and 300–450 m^2/g) was commercial purchased from Qingdao Yuminyuan Silica Gel Reagent Factory, China. SDBS solution was used as received. All aqueous solutions were prepared in 18 MΩ water obtained by purification of deionized water with a Millipore Milli-Q system.

Synthesis of SiO_2/PPy nanocomposite

An aliquot of 2 mL (2.8 g) pyrrole (Py) monomer was dissolved in deionized water to form 300 mL uniformly dispersed solution at ambient temperature. 5.6 g SiO_2 ultrafine powder was added to the Py monomer solution with a stirring speed of 450 r min^{-1} in order to disperse the SiO_2 particles uniformly. Then, 3 g SDBS and 100 mL 1 M $FeCl_3$ solution was added slowly to the above mixture solution consisting of Py monomer and SiO_2 ultrafine particles for the in situ polymerization of PPy. The half-product was vacuum filtered and washed with deionized water to remove impurities and polymers with low-molecular weight. Finally, the resultant product was dried under vacuum at 80 °C for 5 h to obtain a solid stated SiO_2/PPy nanocomposite.

Measurement of conductivity

For the measurement of conductivity, all test samples were prepared in pellet form (diameter: 13 mm, thickness: 1 mm) at pressure of 14 MPa using a Carver model C Press [26]. Four probes method was used to measure the electrical conductivity of the obtained SiO_2/PPy nanocomposites.

Environmental stability

The samples with different preparation conditions were displayed at room temperature and humidity of 35% for days and the conductivities were measured.

Characterizations

Micromorphology of SiO_2/PPy nanocomposite was observed by using JSM-6700F field emission scanning electron microscopy (FESEM). The sample was mounted on metal stub, coated with gold, its surface was observed and photographed by a SEM. The molecular structure of the nanocomposite was identified by IR spectroscopy on a Nicolet Impact 410 FTIR spectrophotometer using KBr pellets. CV measurements of the SiO_2/PPy nanocomposites were performed with a three-electrode electrochemical cell using a CHI660C potentiostat. In acetonitrile solution containing 0.1 M $LiClO_4$ as the supporting electrolyte and 10 mM LiI, 1 mM I_2, this system consisted of SiO_2/PPy samples as the working electrode with the same dimension, a 1.5 mm-diameter platinum foil as the counter electrode, and an Ag/AgCl as the reference electrode.

Results and discussion

Characterizations of the SiO_2/PPy nanocomposite

Figure 1 shows the SEM image of the SiO_2/PPy nanocomposite prepared by aqueous polymerization method. It is clear that the size of SiO_2 particles is approximately 8–10 nm, which is consistent with raw material. PPy nanoparticles with an average diameter of < 5 nm are dispersed in SiO_2 uniformly. From SEM, we can also find that the structure of the nanocomposite is loose which is

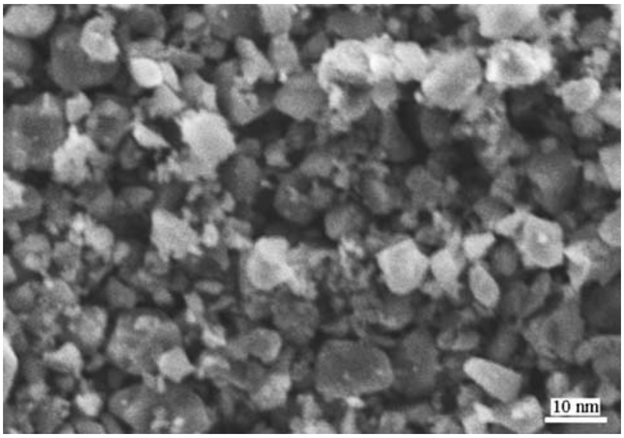

Fig. 1 SEM image of the SiO_2/PPy nanocomposite (Preparation conditions: $FeCl_3$ 0.1 M, Py 2.8 g, SiO_2 8.4 g, SDBS 2.5 g, reaction at 25 °C for 7 h)

favorable for the improvement of electrocatalytic activity. The picture does not show any aggregation of PPy. The homogeneous dispersion of PPy in SiO_2 provides the possibility of high conductivity at low PPy dosages.

Infrared spectrography is a useful technique in characterizing structures of materials. From the micro-transformations in FTIR spectra, we can detect the changes in structures and analyze the potential mechanism subsequently. FTIR spectra of SiO_2 particles and SiO_2/PPy nanocomposite in KBr are performed using an Impact 410 spectrometer. In Fig. 2, the absorption peaks at 3,450 cm^{-1} and 1,640 cm^{-1} are attributed to –OH stretching and bending, respectively. Band at 1,093 cm^{-1} corresponds to Si–O–Si dissymmetrical stretching, 805 cm^{-1} is attributed to Si–O–Si symmetrical stretching, 961 cm^{-1} is for Si–OH. In the IR spectrum of PPy, the absorption peaks at 1,551 cm^{-1} is for $C = C$ stretching, 1,465 cm^{-1} is for C–C stretching, 673 cm^{-1} belongs to SO_3^{2-}. The appearance of SO_3^{2-} reveals that SDBS has doped in the backbone of PPy. 1,322 cm^{-1} is for = C–N stretching and 875 cm^{-1} is the result of C–H stretching in contraposition of benzene ring. Where the intensity ratio of the absorption peaks at 1,551 cm^{-1} to 1,465 cm^{-1} (I_{1551}/I_{1465}) is related to conjugate degree of PPy chains. Compared with the two spectra, the intensity of absorption peaks at 3,450 cm^{-1} and 1,640 cm^{-1} corresponding to –OH stretching and bending of absorbed H_2O in SiO_2 weakens in SiO_2/PPy nanocomposite. The absorption peak at 961 cm^{-1} corresponding to Si–OH has transferred to 984 cm^{-1} in SiO_2/PPy. The changes of peak position and intensity reveal that SiO_2/PPy nanocomposite is not a simple mixture of PPy and SiO_2, some chemical interactions have occurred between the active sites in PPy and SiO_2 [27].

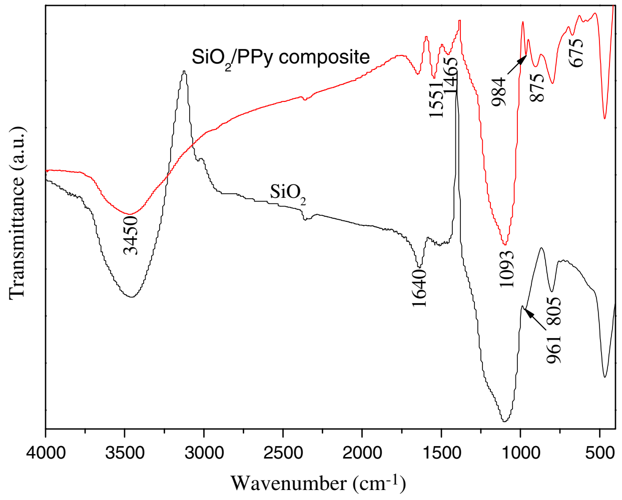

Fig. 2 FTIR spectra of SiO_2 particle and SiO_2/PPy nanocomposite (Preparation conditions: $FeCl_3$ 0.1 M, Py 2.8 g, SiO_2 8.4 g, SDBS 2.5 g, reaction at 25 °C for 7 h)

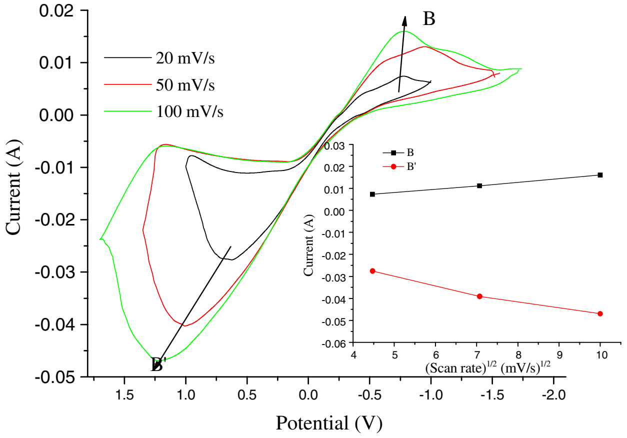

Fig. 3 Cyclic voltammograms for the SiO_2/PPy nanocomposite in acetonitrile solution of 0.1 M $LiClO_4$, 10 mM LiI, 1 mM I_2 with different scan rates (from inner to outer: 20, 50, and 100 mV s^{-1}, respectively). The Preparation conditions: $FeCl_3$ 0.1 M, Py 2.8 g, SiO_2 8.4 g, SDBS 2.5 g, reaction at 25 °C for 7 h

Cyclic voltammetry was carried out in an N_2 purged acetonitrile solution. A SiO_2/PPy nanocomposite electrode was used as working electrode. A Pt coil as the counter electrode, and an Ag/AgCl electrode as reference electrode. The electrolyte was the acetonitrile solution containing 0.1 M $LiClO_4$ as the supporting electrolyte and 10 mM LiI, 1 mM I_2 as the redox couple. Figure 3 shows the CVs of the SiO_2/PPy nanocomposite at different scan rates in acetonitrile solution of 0.1 M $LiClO_4$, 10 mM LiI, and 1 mM I_2. All samples demonstrate electrochemical activity, which is characterized by the typical reduction and oxidation responses. The cathodic peak gradually and regularly shifts to the negative direction and the corresponding anodic peak shifts to the positive direction with increasing scan rate. The good linear relationship with various scan rates indicates the diffusion limitation of the redox reaction on SiO_2/PPy electrode, which may be connected with transport of iodide species out of the SiO_2/PPy electrode surface [28, 29]. This phenomenon shows the adsorption of iodide species is little affected by the redox reaction onto the SiO_2/PPy electrode surface, and this also suggest that no specific interaction between I_2/I^- redox couple and SiO_2/PPy electrode [28, 30]. The excellent electrochemical properties, simple preparation procedure, and inexpensive cost allow the SiO_2/PPy nanocomposites to be applied in electric and photoelectrical devices.

Influence of $FeCl_3$ dosage on conductivity of the nanocomposites

It is well known that dosage is a key factor in effecting the electrical properties of SiO_2/PPy nanocomposite. The influence of $FeCl_3$ dosage on the conductivity of SiO_2/PPy nanocomposite is shown in Fig. 4. The electrical

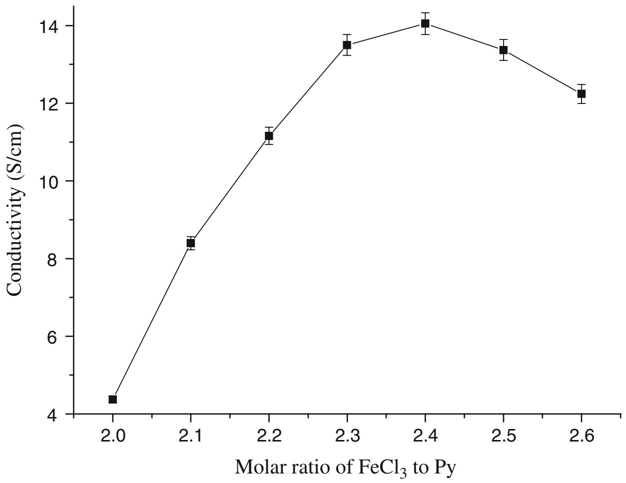

Fig. 4 Conductivity of the nanocomposite versus $FeCl_3$ dosage (Preparation conditions: SiO_2 8.4 g, Py 2.8 g, SDBS 3 g, reaction at 25 °C for 7 h)

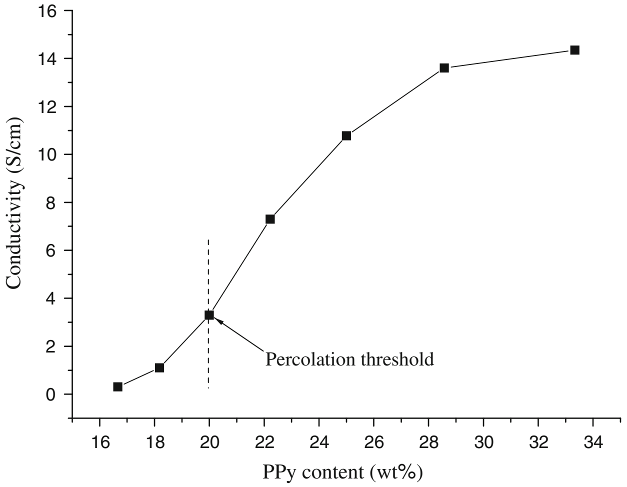

Fig. 5 Conductivity of the nanocomposite versus PPy content (Preparation conditions: $FeCl_3$ 0.1 mol, Py 2.8 g, SDBS 2.5 g, reaction at 25 °C for 7 h)

conductivity of the nanocomposite increases with increase of $FeCl_3$/pyrrole molar ratio in the range of 2.0–2.4, beyond a molar ratio of 2.4, conductivity of the nanocomposite decreases gradually.

It is believed that the conduction of SiO_2/PPy nanocomposite comes from PPy chain. A longer PPy л conjugated chain will result in a higher conductivity [31]. The influence of л conjugated chain length on conductivity can be expressed as follows:

$$\sigma = \frac{f(\infty)q^2L^3}{36\mu_0^3K_2} \qquad (1)$$

where σ is conductivity, $f(\infty)$ is the infinite-chain hopping frequency, q is the charge per carrier, L is л conjugated chains length, μ_0 is the length of Py monomer, and K_2 is a parameter related to energy.

Equation 1 is introduced to explain the effect of dopant dosage on conductivity (σ). From the equation, we can see that the σ mainly depends on the length of conjugated chains (L), because of the direct relationship between σ and cube of L. At a lower dopant dosage, the PPy chains are produced with oligomer which results in a shorter molecular chain. In the case of much higher dopant concentration, such as higher than 2.4 for $FeCl_3$/Py molar ratio, the over oxidation of Py will make the longer PPy chains broken to shorter ones. Much lower or higher dopant dosages can not form a long L, so, the σ decreases in these conditions. In our conditions, the molar ratio of $FeCl_3$/Py at 2.4 is the better.

Influence of PPy content on conductivity of the nanocomposites

The relation between the conductivity and PPy content in nanocomposite was depicted in Fig. 5. It can be seen that conductivity gradually increases with increasing PPy content. The conductivity of SiO_2/PPy nanocomposites at PPy content of 16.67 wt% is 0.31 S cm^{-1}, and dramatically increases from 3.3 to 14.343 S cm^{-1} when the PPy content increases from 20 to 33.33 wt%. It is well known that a highly extended-chain conformation of PPy plays an important role in the conductivity of the composite. In this respect, increasing conducting PPy content means the PPy chains can be highly oriented and extended, so the conductivity increases. According to Fig. 5, to obtain a SiO_2/PPy composite with higher conductivity, the PPy content should preferably be around 33 wt%.

The SiO_2/PPy nanocomposite prepared by aqueous solution polymerization shows a typical percolation phenomenon in terms of electrical conductivity values as a function of PPy content. It has been reported that the percolation phenomenon occurs in polymer matrix conducting composites and percolation theory is an effective technique [32–36]. The excitation of percolation phenomenon attributes to the formation of PPy conducting channels. It is acceptable that the extended PPy chains disperse in SiO_2 matrix and connect each other to form a conducting network. Conduction of electrons is proceeded along the PPy conducting channels. In the case of lower PPy content, such as lower than 20 wt%, the dispersed PPy chains cannot link each other which results in the breakage of channels. In our system, the percolation phenomenon is excited when the PPy content is around 20 wt%.

Influence of SDBS on conductivity of the nanocomposites

As is shown in Fig. 6, the conductivity of SiO_2/PPy nanocomposite increases with SDBS ranging from 1.5 to

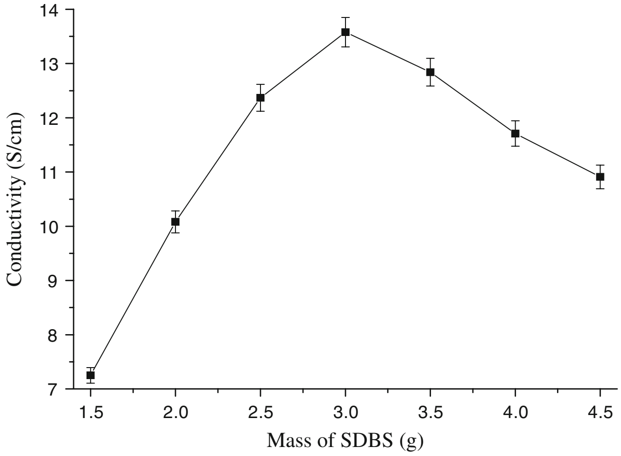

Fig. 6 Conductivity of the nanocomposite versus SDBS amount (Preparation conditions: $FeCl_3$ 0.1 mol, Py 2.8 g, SiO_2 8.4 g, reaction at 25 °C for 7 h)

3 g. Beyond SDBS of 3 g, the conductivity gradually decreases. Since the conduction of electrons along PPy chains can be optimized by the negative ions in SDBS, a conductivity increasing is induced [37]. Much more dopant makes negative ions enrich in PPy chains, which leads to an instability of conjugated chains for the repulsion force. Thus electron conduction is blocked, the result is decline of conductivity. Under our conditions, PPy chains are distributed orderly and conducting structures are perfect at the SDBS dosage of 3.0 g.

Influence of reaction temperature and time on conductivity of the nanocomposites

The reaction temperature and time also affect the structure and conductivity of SiO_2/PPy nanocomposite. From Fig. 7, we can see that the conductivities of different temperature synthesized nanocomposite all increase and then decrease with elongation of reaction time. And the nanocomposite synthesized at higher temperature reaches its highest conductivity is a shorter reaction time. This phenomenon can be interpreted by the general rule of chemical reactions in the Eq. 2.

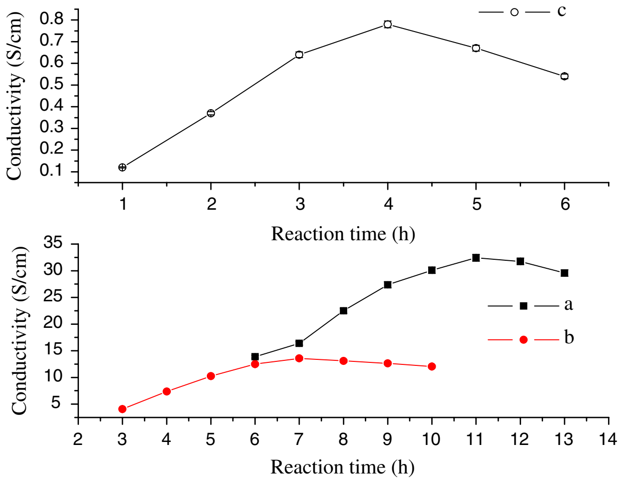

Fig. 7 Conductivity of the nanocomposite versus reaction time and temperature (a. 0 °C, b. 25 °C, and c. 50 °C). Preparation conditions: $FeCl_3$ 0.1 mol, Py 2.8 g, SiO_2 8.4 g, SDBS 3 g

$$\mathrm{n(pyrrole)} \xleftrightarrow[\text{in situ polymerization}]{FeCl_3+SDBS+SiO_2} SiO_2/\mathrm{PPy} + Q \qquad (2)$$

Proper reaction time is necessary for polymerizing extended PPy chains, much longer oxidation time will result in the over oxidation of Py monomer and breakage of PPy conjugated chains. From Eq. 1, the conductivity of the nanocomposite instead decreases. Since the polymerization of PPy is an exothermic reaction, the synthesis at higher temperature will produce more PPy with short conjugated length which is unfavorable for the improvement of conductivity. In order to obtain the nanocomposites with high conductivity, the synthesis should be operated at lower temperature, as has been approved in polyaniline systems by other groups [38, 39].

Environmental stability of the nanocomposites

Due to the hydrophilic nature of the doped PPy, it is soluble or dispersible in water. And the hydrophilicity increases with increasing length of hydrophilic chain in the dopant, also leads to increase in its solubility in water [40]. In actual application, it is important that the composite keeps its conductivity without declining during storage. In order to investigate conductivity stability of the SiO_2/PPy nanocomposite, the samples with different preparation conditions [reacted at 0 °C for 11 h (sample a), at 25 °C for 7 h (sample b), at 50 °C for 4 h (sample c)] were displayed at room temperature and humidity of 35% for days and the conductivities were measured. From Fig. 8, the conductivity of the nanocomposites remains fairly stable but the stability is influenced by the polymerization reaction temperature. For the three samples (a), (b), and (c), their conductivities were kept at 90.6, 82.4, and 61.2% of the original values, respectively, after 50 days. The superior stability of sample (a) may be due to the fact that sample (c) is prepared at a higher temperature for a longer reaction time, inducing more side reactions and allowing more by-products to occur, causing a decline in stability.

Conclusions

In summary, SiO_2/PPy conducting nanocomposite was prepared by polymerizing pyrrole in aqueous solution with ultrafine SiO_2 powder in the presence of SDBS as dopant

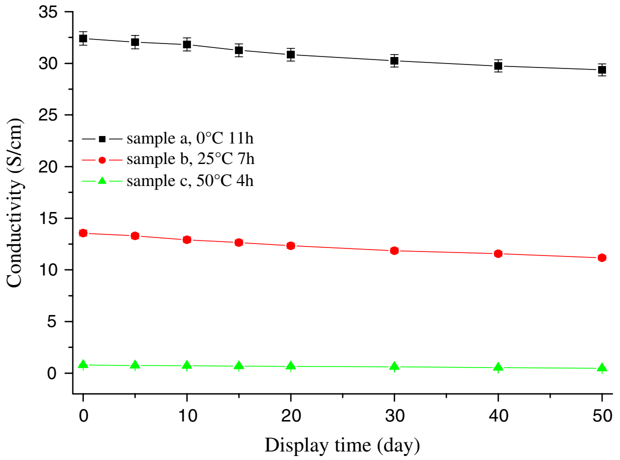

Fig. 8 Influences of display time on conductivity of the nanocomposites at 25 °C (Preparation conditions: $FeCl_3$ 0.1 mol, Py 2.8 g, SiO_2 8.4 g, SDBS 2.5 g)

and $FeCl_3$ as oxidant agent. After optimum reaction, a conductivity of 32.41 S cm^{-1} and percolation threshold of 20 wt% were obtained in the SiO_2/PPy nanocomposite. Cyclic voltammograms of I_2/I^- system measurement revealed that the SiO_2/PPy nanocomposite had small charge-transfer resistance and high electro catalytic activity for the I_2/I^- redox reaction. The SiO_2/PPy nanocomposites presented a good environmental stability. The excellent electronical and electrochemical properties, good stability, simple preparation procedure, and inexpensive cost allow the SiO_2/PPy nanocomposites to have potential use in electric and photoelectrical devices.

Acknowledgements The authors thank for jointly support by the National Natural Science Foundation of China (No. 50572030), the Specialized Project of Fujian Province (Nos. 2005HZ01-4, 2007HZ0001-3), the Key Project of Chinese Ministry of Education.(No. 206074), and Specialized Research Fund for the Doctoral Program of Chinese Higher Education (No. 20060385001).

References

1. Gangopadhyay R, De A (2000) Chem Mater 12:608
2. Liu Y, Chu Y, Yang L (2006) Mater Chem Phys 98:304
3. Kang TS, Lee SW, Joo J (2005) Synth Met 153:61
4. Liu L, Zhao CJ, Zhao YM (2005) Eur Polym J 41:2117
5. Mabrook MF, Pearson C, Petty MC (2006) Sensor Actuat B 115:547
6. Liu YC, Lee HT, Yang SJ (2006) Electrochim Acta 51:3441
7. Armes SP, Aldissi M, Agnew SF (1989) Synth Met 28:837
8. Maeda S, Armes SP (1995) Synth Met 69:499
9. Radhakrishnan S, Deshpande SD (2001) Mater Lett 48:144
10. Erlandsson R, Inganas O, Lundstrom I (1985) Synth Met 10:303
11. Audebert P, Aldebert P, Pineri M (1989) Synth Met 32:1
12. Bhattacharya A, De A (1996) Prog Solid State Chem 24:141
13. Shen Y, Wan M (1998) Synth Met 96:127
14. Partch R, Gangolli SG, Matijevic E, Cai W, Arajs S (1991) J Colloid Interface Sci 144:27
15. Mehrotra V, Keddie JL, Miller JM, Giannelis EP (1991) J Non-Cryst Solids 136:97
16. Yoneyama H, Shoji Y (1990) J Electrochem Soc 137:3826
17. Liu C, Maruyama T, Yamamoto T (1993) Polym J 25:363
18. Han G, Yuan J, Shi G (2005) Thin Solid Films 474:64
19. Ferrer AN, Kaempgen M, Skakalova V (2004) Diam Relat Mater 13:256
20. Mravcakova M, Boukerma K, Omastová M (2006) Mater Sci Eng C 26:306
21. Boukerma K, Piquemal JY, Chehimi MM (2006) Polymer 47:569
22. Trueba M, Trasatti SP, Trasatti S (2006) Mater Chem Phys 98:165
23. Tandon RP, Tripathy MR, Arora AK (2006) Sensor Actuat B 114:768
24. Papathanassiou AN, Grammatikakis J, Sakellis I (2005) Synth Met 150:145
25. Nakayama M, Yano J, Nakaoka K (2003) Synth Met 138:419
26. Parvatikar N, Jain S, Khasim S (2006) Sensor Actuat B 114:599
27. Maeda S, Armes SP (1993) J Colloid Interface Sci 159:257
28. Saito Y, Kubo W, Kitamura T et al (2004) J Photochem Photobiol A 164:153
29. Biallozor S, Kupniewska A (2000) Electrochem Commun 2:480
30. Hauch A, Georg A (2001) Electrochim Acta 46:3457
31. Carrasco PM, Grande HJ, Cortazar M (2006) Synth Met 156:420
32. Shekhar S, Prasad V, Subramanyam SV (2006) Carbon 44:334
33. Li JR, Xu JR, Zhang MQ (2003) Carbon 41:2353
34. Emmerich FG, de Sousa JC, Torriani IL et al (1987) Carbon 25:417
35. Malmonge LF, Mattoso LHC (1995) Polymer 36:245
36. Ghosh P, Chakrabarti A (2000) Eur Polym J 36:1043
37. Song MK, Kim YT, Kim BS (2004) Synth Met 141:315
38. Yan H, Toshima N (1995) Synth Met 69:151
39. Cao Y, Andreatta A, Heeger AJ et al (1989) Polymer 30:2305
40. Geng YH, Sun ZC, Li J (1999) Polymer 40:5723